

---

# Wireless Sensor Networks for Activity Monitoring using Multi-sensor Multi-modal Node Architecture

Peter Hung<sup>†</sup>, Muhammad Tahir, Ronan Farrell, Seán McLoone and Tim McCarthy

*Department of Electronic Engineering  
Institute of Microelectronics and Wireless Systems  
National University of Ireland Maynooth  
Maynooth, Co. Kildare, Ireland*

E-mail: <sup>†</sup>phung@eeng.nuim.ie

---

*Abstract* — A multi-sensor, multi-modal sensor node for human and vehicle activity monitoring is designed and developed. As a first step to achieve our objective, we have used a dual pyroelectric IR (PIR) sensor system for human activity monitoring. The sampled data from two PIR sensors, under laboratory conditions, is first processed individually to determine the event window size, which is then fed to simple algorithms to determine direction and potentially measure speed of passing humans. We also show that human count can be obtained for some special scenarios. Preliminary results of our experimentation show the effectiveness of the simple algorithms proposed.

*Keywords* — Multi-sensor, activity monitoring, data fusion, pyroelectric IR.

---

## I INTRODUCTION

Human detection and motion tracking have always been of much interest for a large class of applications including surveillance, navigation as well as smart environments. Conventionally, tracking is performed using cameras with large data processing overheads to extract features, for instance, number of people, position and direction of motion [1]. Even if these solutions are accurate, they have high cost and require significant infrastructure deployment. On the other hand, pyroelectric infrared (PIR) based sensors exploit pyroelectricity to detect an object that is not at thermal equilibrium with the surroundings [2]. PIR sensors are widely used in commercial applications to detect human presence to trigger security alarms. In addition, these sensors have also found applications in thermal imaging, radiometry, thermometry as well as biometry [3], [4].

A single PIR sensor is used widely in security related applications to detect an intruder [5]. Multiple PIR sensors are used to achieve coverage [6], to assist video surveillance [7] as well as to perform tracking [8]. The authors in [5] have used PIR sensors to differentiate a still person from its background. The authors in [6] have employed four PIR sensors to achieve 360° coverage while performing human detection. In their

implementation all four PIR sensor outputs are combined by a summing amplifier before being fed to an analog-to-digital converter (ADC). Consequently, individual sensor outputs are not accessible to the signal processing algorithm. This limits the capabilities of the sensor node to human detection. A video surveillance system using multi-modal sensor integration is proposed in [7], in which a multiple camera tracking system is integrated with a wireless sensor network equipped with PIR sensors.

Human tracking using PIR sensors in a hierarchical network involving sensing modules acting as slaves, a synchronization and error rejection module as a master and a data fusion module termed as host, is discussed in [8]. This is achieved by designing a geometric sensor module with multiple PIR sensors, each equipped with a Fresnel lens array to obtain a spatially modulated field of view. In addition to tracking, PIR sensors can also be used to detect, differentiate and describe human activity. In [9] the authors have used PIR enabled sensor nodes with information exchange with the base station to determine the direction, speed and number of people. The work in [9] is further extended in [10] to perform distance estimation in hallway like scenarios using two PIR enabled nodes installed on opposite sides of the hallways.

The approaches discussed above are limited due to the accurate time synchronization required across sensor nodes and the communication overhead involved. Our proposed approach addresses these issues by integrating two PIR sensors at each sensor node providing accurate timing for the sampled data from the two PIR sensors and eliminating associated communication overhead.

## II HUMAN DETECTION AND COUNTING

Usually PIR sensors are designed as part of an overall intrusion detection system, where alarms are activated whenever a PIR output exceeds a predefined threshold. Multiple PIR sensors along with simple signal processing algorithms can be used for obtaining parameters of interest. This paper attempts to obtain the parameters of interest for human activity monitoring, by employing simple data analysis techniques, once the sampled data from only a single node is obtained. The first step towards this objective involves distinguishing each individual object as it enters the field-of-view (FOV) of the sensor. The next step involves counting the number of human beings passing through the sensor FOV. However, there are two issues in this step when a single PIR sensor is used. The first issue is related to the distance between the object and the nearest sensor. If the moving object is closer to the sensor, the resulting duration of excitation (i.e. event window) will be shorter. Secondly, it would be difficult to differentiate between the scenarios of 1) two people walking close by with their individual sensor excitations overlapping and; 2) A person walking at half the speed of two close by people scenario.

A possible solution is to incorporate two sensors, instead of one, to extract the parameters of interest. There are several advantages of processing the outputs of both PIR sensors jointly. First, the speed of the moving object can be calculated more reliably. Secondly, the direction of the moving object can easily be determined from the first step. In addition, it is also possible to count reliably the number of people passing by for some scenarios. This will now be elaborated on in more detail.

Consider an object moving at constant speed  $v$  and being detected by a PIR sensor for the time interval  $t$ . If there are two sensors placed close by on the same node such that the midpoints of their FOVs are separated by a distance  $d$  as shown in Fig. 1, then

$$d = \int_{t_A}^{t_B} v dt, \quad (1)$$

where  $t_A$  and  $t_B$  correspond to the time instances when the moving object reaches the FOV midpoints corresponding to the center of event window of sensors A and B, respectively. A similar approach is proposed in [11] for traffic monitoring, with the exception that two physically separated nodes are used for that purpose. The parameter  $\theta$  is used to adjust the overlap of the respective FOVs of the two sensors. If it is assumed that a human is walking in a narrow pathway

(of width  $c$  as depicted in Fig. 1), then the assumption of approximately constant  $d$  is valid and as a result both sensors produce approximately similar output, regardless of how the moving object approaches the detector. For this fixed value of  $d$  the expression in (1) can be rewritten as

$$v = \frac{d}{t_B - t_A} \quad (2)$$

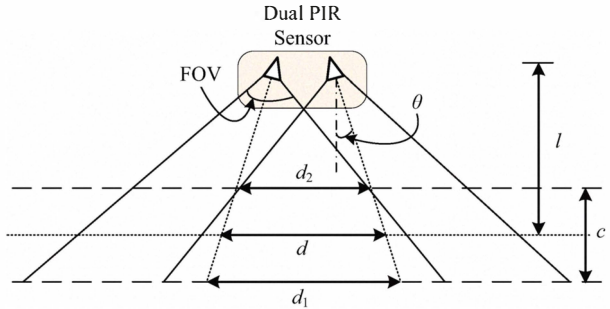


Fig. 1: Physical arrangement of two PIR sensors and their FOV. To limit the error due to relative proximity of the human object to the sensor we assume that  $c/l \ll 1$  leading to  $d \approx d_1$  and  $d \approx d_2$ .

The result in (2) can be used to estimate the speed of moving objects because  $d$  is constant. Additionally, the sign of  $v$  can be used to determine the direction of the moving object under observation.

There are situations where more than one human being, for instance multiple persons having a conversation and walking in a queue, are passing through the FOV of the sensor and are close enough to one another that their respective PIR sensor outputs overlap. However, as excitation duration, and as a result event window, are proportional to human body ‘thickness’, which is constant under the assumption of an approximately fixed  $d$ , the number of persons consecutively approaching the detector can be enumerated from the event window duration and the corresponding walking speed  $v$ .

In practice, to obtain a reliable estimate of  $v$ , the midpoint of FOV for the two sensors must be sufficiently separated to obtain a larger denominator in (2). At the same time, it cannot be made very large due to the fact that each sensor has a limited range. More details on the hardware design will be presented in the next Section.

## III NODE ARCHITECTURE

Our sensor node is designed to achieve local intelligence using a multi-modal, multi-sensor architecture, while minimizing the inter-node data transfers to improve its power efficiency. To achieve this, some parameters are sensed using more than one sensor providing diversity enabling us to extract some of the desired features, which cannot be obtained using a single sensor. The block diagram in Fig. 2(a) provides the architectural details of our sensor node with different subsystems and the respective data exchange interfaces. The hardware realization of our sensor node

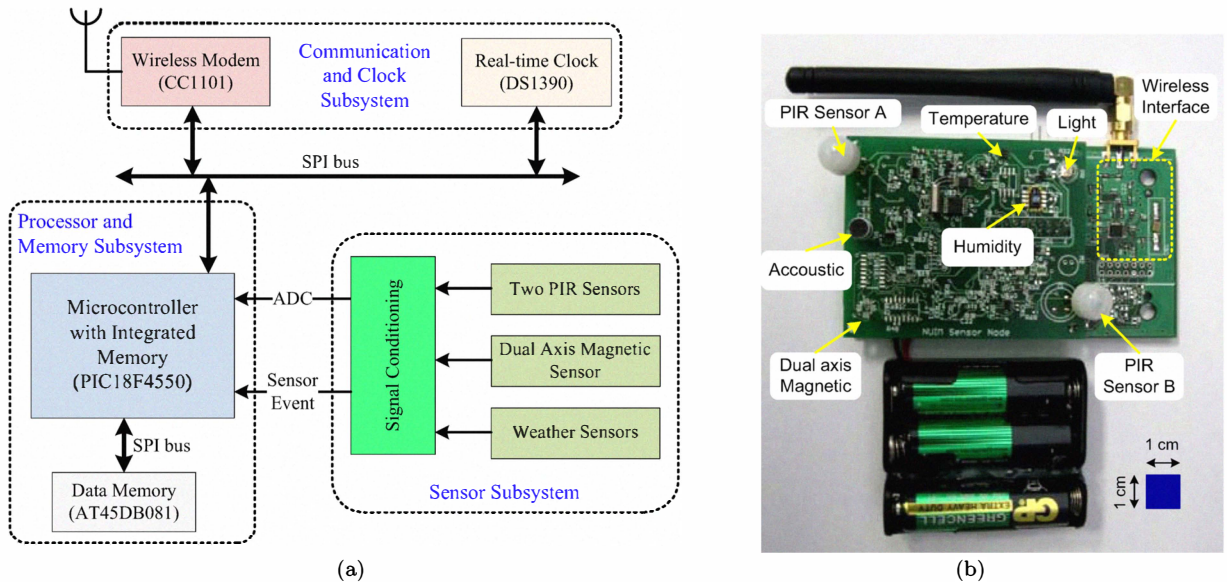


Fig. 2: (a) Sensor node architecture block diagram with different subsystems and the corresponding data exchange interfaces. (b) Picture of node hardware with sensor board mounted on top of the processor and communication board.

using a modular approach is depicted in Fig. 2(b). The sensor module having dimensions  $60 \text{ mm} \times 70 \text{ mm}$  is mounted on top of a processor and communication module with dimensions  $60 \text{ mm} \times 100 \text{ mm}$ . The processor and communication module is also equipped with a USB interface so that the node can be used as a host, which results in a relatively larger node size. We emphasize that the node size can be reduced by removing the USB interface for the non-host sensor nodes. Next the building blocks of our sensor node is briefly described.

#### a) Sensor Subsystem

The objective of the sensor subsystem is to monitor moving objects i.e. pedestrians and vehicles, in a reliable manner. For each sensed parameter, the sensor along with its signal conditioning electronics constitutes the corresponding sensor module. Different sensor modules are interfaced to the processor using an analog multiplexer. Digital power control is provided to selectively turn on a sensor module leading to power consumption minimization. The individual sensor modules for monitoring pedestrians and vehicles are as follows.

- **Pedestrian Monitoring:** The PIR sensor is at the heart of achieving the pedestrian monitoring objective. The signal conditioning block for each of the PIR sensors consists of two cascaded filtering/amplifier stages with an overall gain in excess of 60 dB. The two sensors are mounted on the board in such a way that they have partial overlap in their respective FOVs. The sensor performance is limited due to its high susceptibility to sunlight and its long startup time ( $> 1000 \text{ ms}$  [12]).
- **Traffic Monitoring:** For the purpose of traffic monitoring, we consider magnetic and PIR sen-

sors jointly to achieve vehicle detection, travel direction, vehicle classification and speed estimation. Joint processing of two sensor inputs allows us to differentiate vehicles from humans, as the magnetic sensor only responds to passing vehicles. Due to the special response characteristics of each of these sensors different algorithms for detection/classification and parameter extraction may be required. On the other hand, a sensor capable of sensing two different classes of objects (e.g. PIR can be used for detecting both vehicles as well as pedestrians), needs to be complemented by an intelligent algorithm and/or a sensor to achieve multi-parameter extraction.

Table 1 lists the selected sensors and their key features for each of the sensed parameter. In contrast to multiple special purpose sensor nodes distributed spatially and lacking accurate time synchronization, our multi-modal multi-sensor node, with simplified local data processing algorithms should achieve better performance by jointly processing data from different sensors.

#### b) Communication and Clock Subsystem

The communication interface is based on the CC1101, sub 1 GHz ISM band, radio transceiver. The CC1101 radio is interfaced to a hardware interrupt to wakeup the processor upon the arrival of an incoming packet to reduce node power consumption. The transceiver can achieve a 10 dBm transmit power without an external power amplifier. A hardware based real time clock (RTC) source at each sensor node is used for periodic node wakeup. This is in addition to the event based wakeups from human and traffic monitoring sensors and allows the processor to enter into deep sleep modes. The RTC is also used to reduce the time synchronization overhead due to its better accuracy, compared to software based solutions, with

Table 1: Sensor parameters

Sensor	Manufacturer Part No.	Parameters	Remarks
PIR	IRA-E710ST0	$\pm 45^\circ$ FOV, $4.3\text{mV}_{p-p}$	Requires Fresnel lens
Magnetometer	HMC1052L	dual axis, 5 MHz BW	0.1 % duty cycle, $2\ \mu\text{s}$ , $.5\ \text{A}$ set/reset current pulse

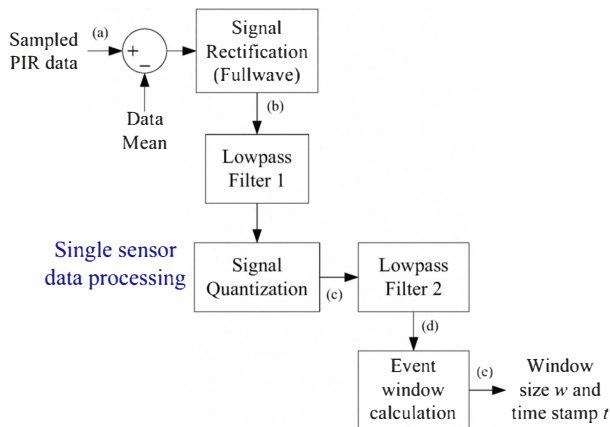


Fig. 3: Block diagram of event window detection (EWD) algorithm from a single PIR sensor sampled at 10 ms.

minimal cost overhead.

### c) Processor and Memory Subsystem

An 8-bit PIC18LF4550 microcontroller is chosen with 32 Kbytes flash, 2 Kbytes of RAM, 48 MHz clock frequency and sleep mode current down to  $0.1\ \mu\text{A}$ . The microcontroller has a total of thirteen channels of 10-bit ADC and 3 external interrupts. An 8 Mbit serial flash memory from Atmel, AT45DB081D, is provided at each sensor node for temporary data storage.

## IV DATA ACQUISITION AND PROCESSING

### a) Data Acquisition

The data is either sampled directly or amplified before sampling depending on the signal magnitude at the sensor output. Digital potentiometers are used for dynamic amplifier gain control to improve performance range. Periodic sampling with a uniform sampling rate of 0.1 kHz is used for sampling data from the two PIR sensors simultaneously. The sampling rate is chosen to cover a wide range of pedestrian walking speeds.

### b) Data Processing

To facilitate human detection and motion tracking, the following data processing is proposed. The duration of each sensor excitation, including the start and end times, should first be found. Then, the number of people, as well as their direction of passage through the sensor node viewpoint at a given time interval, can be deduced.

- **Duration of Excitation or Event Window Calculation:** The block diagram shown in Fig. 3 outlines the general steps of event window detection (EWD) algorithm to find the duration of sensor

excitation in the form of event window  $w$ . As can be seen from Fig. 3, the first low-pass filter is used to remove the background noise inherent in the sensor signals and can be different for indoor and outdoor situations. Currently, a third-order Butterworth filter with a cut-off frequency of 10 Hz is employed. The filtered and full-wave rectified signal is then quantised prior to application to second low-pass filtering. Each individual temporal sensor excitation is segmented by the second first-order Butterworth low-pass filtering with a 1.5 Hz cut-off, which creates an ‘enclosure’ envelope for each excitation. Finally, a gradient search on the binary signal is performed in each enclosure to detect the event window start and end times, and hence the duration of sensor excitation.

During testing, a minimum distance of  $l$  (Fig. 1), currently set at 2 m, is used to prevent saturated sensor excitation. Also, it is found that the absolute mean sensor outputs provide more accurate timing information of node excitation compared to zero-mean outputs. This is because a more effective low-pass filtering is possible for non-negative signals compared to ones with fluctuations above and below the mean value.

- **Human Counting:** Due to the use of two PIR sensors in the sensor node, the approaching direction of a human with respect to the sensor node can readily be checked by determining the sign of the following expression:

$$\phi = \frac{t_A^{(e)} - t_A^{(s)}}{2} - \frac{t_B^{(e)} - t_B^{(s)}}{2}, \quad (3)$$

where  $s$  and  $e$  are start and end instances of event windows. A positive value of  $\phi$  in (3) suggests a movement from sensors A to B and vice versa. The magnitude of this difference can be used to calculate the speed  $v$  of human motion. Having found  $v$ , and given a fixed  $d$ , the number of people walking past the sensor FOV can be deduced accordingly.

## V RESULTS

This section presents some preliminary results on human activity detection. The different parameters used in our experiments are provided in Table 2. A walking speed of approximately 1 m/s was employed in all cases. Fig. 4 shows the raw outputs from two sensors when a person walks in opposite directions. It can be seen that the excitation window corresponding to the output of Sensor A will appear first (in time) followed by the excitation window for Sensor B when



Table 2: Parameters used in the experimentation.

Parameters	Value
FOV angular deviation $\theta$	$30^\circ$
Sensor to pathway midpoint gap $l$	2.5 m
Width of pathway $c$	1.5 m
Data sampling interval	10 msec

the person walks from left to right in front of the sensors and vice versa when the person walks from right to left. This can be used to determine the direction of motion of the walking person.

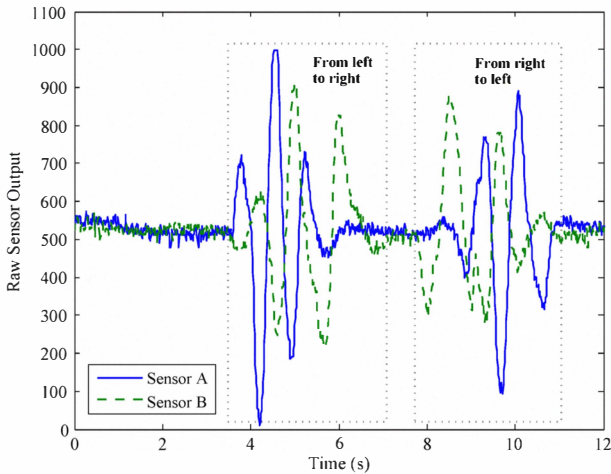


Fig. 4: The two sensor outputs corresponding to a single person walking in opposite directions.

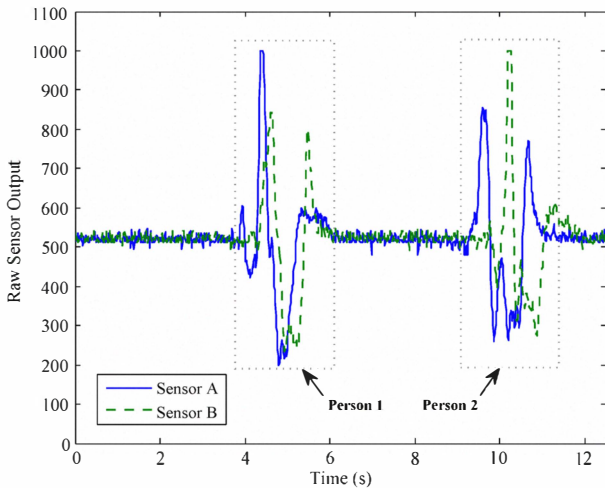


Fig. 5: Sensor outputs in case of two pedestrians walking in the same direction from FOV of sensor A towards that of sensor B.

The signals obtained for the case when two people are walking in the same direction is shown in Fig. 5. This scenario is differentiated from the one in Fig. 4 using the phase delay in the event windows corresponding to the two sensor outputs. When the two people are walking single file in close proximity, the sensor response for each person will partially overlap and the duration of the resulting event window will be larger than that corresponding to a single person.

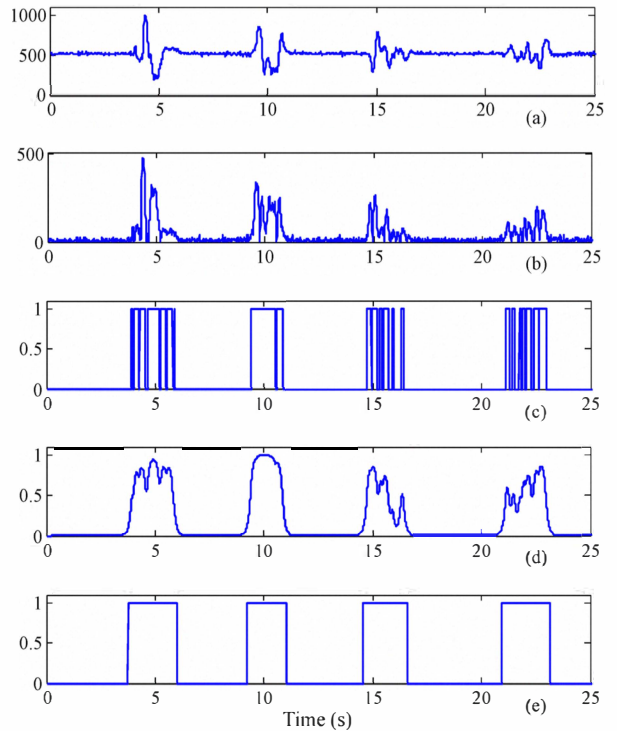


Fig. 6: Actual sampled data from the sensor and the outputs corresponding to different steps performed in executing the EWD algorithm; (a) the raw sensor output from a 10-bit ADC, (b) the output of the first low-pass filter, (c) quantised signal, (d) second low-pass filter output, and (e) the final output in the form of the event window duration estimate.

A threshold is required to make the system robust to fluctuations due to noise.

Fig. 6 shows the outputs corresponding to different steps of the EWD algorithm described in Fig. 3. The signal in Fig. 6(a) is the raw sensor output obtained from a 10-bit ADC. Fig. 6(b) is the output after application of full-wave rectification. After the first low-pass filtering, used to remove the high frequency noise, the quantised output (thresholded at 50) is shown in Fig. 6(c) and the output of the second low-pass filter is shown in Fig. 6(d). The output in Fig. 6(e) is the event window duration obtained by applying thresholding at 0.1. As discussed in Section IV, this event window duration and its corresponding start and end times can be used to extract the direction of motion as well as number of the people walking in a queue.

## VI DISCUSSION AND CONCLUSIONS

We have designed and developed a multi-sensor, multi-modal sensor node for human and vehicle activity monitoring. A dual pyroelectric IR (PIR) sensor system for human activity monitoring is proposed. The data from two PIR sensors are first processed individually to determine the event window size, and then fed to simple algorithms to determine the direction of motion and speed of passing humans. The system can also provide human count for some specific scenarios. Our results show the effectiveness of the architecture and the simple algorithms developed for human activity monitoring and suggests that the

system has the potential to complement more complex monitoring networks such as camera networks.

The fixed value of distance  $d$  (Fig. 1) used in evaluating the speed of the object can be a source of error. We plan to address this issue by using the signal strength (in the form of power/energy content or peak value) to calibrate the parameter  $d$  to minimize the error due to variable separation between the sensor and the moving object. Future works will also include evaluation of the potential for detecting vehicles which move at much greater speeds than human beings.

#### ACKNOWLEDGMENT

Research presented in this paper was funded by a Strategic Research Cluster grant (07/SRC/I1168) from Science Foundation Ireland under the National Development Plan. The authors gratefully acknowledge this support.

#### REFERENCES

- [1] Q. Cai, JK Aggarwal, R. Inc, and WA Seattle. Tracking human motion in structured environments using adistributed-camera system. *IEEE Transactions on Pattern Analysis and Machine Intelligence*, 21(11):1241–1247, 1999.
- [2] P. Muralt. Micromachined infrared detectors based on pyroelectric thin films. *Reports on Progress in Physics*, 64(10):1339, 2001.
- [3] C.F. Tsai and M.S. Young. Pyroelectric infrared sensor-based thermometer for monitoring indoor objects. *Review of Scientific Instruments*, 74:5267, 2003.
- [4] J.S. Fang, Q. Hao, D.J. Brady, M. Shankar, B.D. Guenther, N.P. Pitsianis, and K.Y. Hsu. Path-dependent human identification using a pyroelectric infrared sensor and Fresnel lens arrays. *Optics Express*, 14(2):609–624, 2006.
- [5] D. Karuppiah, P. Deegan, E. Araujo, Y. Yang, G. Holness, Z. Zhu, B. Lerner, R. Grupen, and E. Riseman. Software mode changes for continuous motion tracking. *Lecture notes in computer science*, pages 161–180, 2001.
- [6] A. Arora, R. Ramnath, E. Ertin, P. Sinha, S. Bapat, V. Naik, V. Kulathumani, H. Zhang, H. Cao, M. Sridharan, et al. Exscal: Elements of an extreme scale wireless sensor network. In *11th IEEE International Conference on Embedded and Real-Time Computing Systems and Applications, 2005. Proceedings*, pages 102–108, 2005.
- [7] A. Prati, R. Vezzani, L. Benini, E. Farella, and P. Zappi. An integrated multi-modal sensor network for video surveillance. In *Proceedings of the third ACM international workshop on Video Surveillance & sensor networks*, pages 95–102. ACM New York, NY, USA, 2005.
- [8] Q. Hao, D.J. Brady, B.D. Guenther, J.B. Burchett, M. Shankar, and S. Feller. Human tracking with wireless distributed pyroelectric sensors. *IEEE Sensors Journal*, 6(6):1683–1696, 2006.
- [9] P. Zappi, E. Farella, and L. Benini. Enhancing the spatial resolution of presence detection in a PIR based wireless surveillance network. In *IEEE Conference on Advanced Video and Signal Based Surveillance*, pages 295–300, 2007.
- [10] P. Zappi, E. Farella, and L. Benini. Pyroelectric InfraRed sensors based distance estimation. In *IEEE Sensors*, pages 716–719, 2008.
- [11] TM Hussain, AM Baig, TN Saadawi, and SA Ahmed. Infrared pyroelectric sensor for detection of vehicular traffic using digital signal processing techniques. *IEEE transactions on vehicular technology*, 44(3):683–689, 1995.
- [12] P. Dutta, M. Grimmer, A. Arora, S. Bibyk, and D. Culler. Design of a wireless sensor network platform for detecting rare, random, and ephemeral events. In *Proceedings of the 4th international symposium on Information processing in sensor networks*, pages 497–502, 2005.